https://doi.org/10.5194/hess-2023-238
Preprint. Discussion started: 6 November 2023

Hydrology and Earth System Sciences
Open Access
Discussions

Controls on the relatively slow thinning rate of a debris-covered glacier in the Karakoram over the past 20 years: evidence from mass and energy budget modelling of Batura Glacier

Yu Zhu[1,2], Shiyin Liu[1,2,5*], Ben W. Brock[3], Lide Tian[1,2], Ying Yi[1,2], Fuming Xie[1,2], Donghui Shangguan[4], and YiYuan Shen[1,2]

[1] Institute of International Rivers and Eco-Security, Yunnan University, 650091 Kunming, China

[2] Yunnan Key Laboratory of International Rivers and Transboundary Eco-security, 650091 Kunming, China

[3] Department of Geography and Environmental Sciences, Northumbria University, Newcastle upon Tyne, NE1 8ST, UK

[4] Northwest Institute of Eco-Environment and Resources, Chinese Academy of Sciences, Lanzhou 730000, China

[5] International Joint Laboratory of China-Laos-Bangladesh-Myanmar Natural Resources Remote Sensing Monitoring

Corresponding author: Shiyin Liu (shiyin.liu@ynu.edu.cn)

Abstract:

The influence of supraglacial debris cover on glacier dynamics in the Karakoram is noteworthy. However, understanding of how debris cover affects the seasonal and long-term variations in glacier mass balance through alterations in the glacier's energy budget is incomplete. The present study applied an energy-mass balance model coupling heat conduction within debris layers on debris-covered Batura Glacier in Hunza valley, to demonstrate the influence of debris cover on glacial surface energy and mass exchanges during 2000-2020. The mass balance of Batura Glacier is estimated to be -0.262 ± 0.561 m w.e. yr^{-1}, with debris cover reduced 45% of the negative mass balance. Due to the presence of debris cover, a significant portion of incoming energy is utilized for heating debris, leading to a large energy emission to atmosphere via thermal radiation and turbulent sensible heat. This, in turn, reducing the melt latent heat at the glacier surface. We found that the mass balance exhibits a pronounced arch-shaped structure along the elevation gradient, which primarily attributes to the distribution of debris thickness and the impact of debris cover on the energy budget within various elevation zones. Through a comprehensive analysis of the energy transfer within each debris layer, we have demonstrated that the primary impact of debris cover lies in its ability to modify the energy flux reaching the surface of the glacier. Thicker debris cover results in a smaller temperature contrast between debris layers and the ice-contact zone, consequently reducing heat conduction. Over the past two decades, Batura Glacier has maintained a relatively small negative mass balance, owing to the protective effect of debris cover. The glacier exhibits a tendency towards a smaller negative mass balance, with diminishing dominance of ablation in areas with thin debris cover and debris-free parts of the ablation area.

https://doi.org/10.5194/hess-2023-238
Preprint. Discussion started: 6 November 2023

Hydrology and Earth System Sciences
Discussions

1 Introduction

Karakoram Glaciers have maintained a relative stable status under atmospheric warming compared with other High Mountain Asia (HMA) glaciers over past 30 years (Zemp et al., 2019; Nie et al., 2021; Gardelle et al., 2012), a phenomenon which has been referred to as the “Karakoram Anomaly” (Hewitt, 2005). However, due to the influence of topographical and supraglacial features, the rate of glacier change across this region exhibits a distinct spatial heterogeneity. Notably, supraglacial debris plays a key role in mass change on many covered glaciers in the Karakoram. Over the past three decades, a discernible expansion of supraglacial debris has been observed throughout the Karakoram region (Xie et al., 2023), achieving a notable coverage of 21% in select areas such as the Hunza river basin (Xie et al., 2020). Ever since Hewitt (2005) identified the inhibitory effect of supraglacial debris on melt, particularly below 3500m, as a possible explanation for the "Karakoram Anomaly", mapping the changes in the extent and mass changes of debris-covered glaciers has been the focus of several recent studies (e.g., Mölg et al. (2018), Azam et al. (2018), Xie et al. (2020)). Limited research has been devoted to comprehensively exploring the intricate dynamics of mass and heat exchange within the debris in the Karakoram, however.

Supraglacial debris up to a few centimeters thickness generally increases melt due to lowered albedo and increased heat absorption at the surface (Collier et al., 2014), while thicker debris cover can suppress melt rate through insulation (östrem, 1959; Nicholson and Benn, 2006; Bisset et al., 2020). These contrasting effects have been demonstrated by many recent studies (Gardelle et al., 2012; Nuimura et al., 2017; Basnett et al., 2013; Fujita and Sakai, 2014). The reduction of ablation associated with increasing debris thickness down glacier can lead to an inverted mass-balance elevation profile on the debris-covered ablation zone, which has profound implications on the evolution of a glacier under a warming climate (Banerjee, 2017). Some field studies have also identified diverse effects on melt rates of debris cover with different thickness in Karakoram, one particular finding showed that thin debris cover, e.g. 0.5 cm in thickness, does not accelerate ice melting in this region (Muhammad et al., 2020). However, some remote sensing based research proposed while thick debris typically inhibits the melt rate, the overall ablation on a glacier covered in debris can still exhibit a relatively significant magnitude (Kääb et al., 2012). These findings imply that understanding of the process and feedback mechanisms governing ablation of debris-covered glaciers in this region is still incomplete. Therefore, it is important to quantify not only the amplitude of melt under time-variable debris cover but also its role in “Karakoram Anomaly” by assessing the thermal properties of debris layers of different thickness.

Field glaciological and meteorological observations on glaciers in the Karakoram are limited by logistical and political constraints (Mayer et al., 2014; Mihalcea et al., 2008). Consequently, a significant knowledge gap exists for debris thickness and its thermal properties as well as the complex coupling of meteorology with heat exchange over glaciers and in debris layers. A limited number of previous melt process investigations under debris layers, e.g., Juen et al. (2014), Evatt et al. (2015), Muhammad et al. (2020), supported by remote sensing observations and climate reanalysis data, have enabled physically-based numerical modeling to provide insight into thermal dynamics within supraglacial debris. For example, Huo et al. (2021) provided new insights into the relationships between ablation dynamics, surface morphology and debris transport, while Collier et al. (2015) developed understanding of how debris cover affects the atmosphere–glacier feedback processes during the melt season. However, despite these advancements, certain aspects remain insufficiently addressed. Specifically, the seasonal variations and long-term changes in melt patterns, along with the manner in which debris cover exerts its influence on such variations, have not been comprehensively studied. Understanding these dynamics is essential not only for establishing the physical basis of the "Karakoram Anomaly" but also for quantifying the extent to which debris cover contributes to this phenomenon. In this study, we applied an energy-mass balance model coupling heat conduction within debris layers on Batura Glacier in Hunza valley, Karakoram to demonstrate the influence of debris cover on glacial melt. We aim to: (1) reconstruct the long-term mass balance history of the Batura Glacier, a representative debris-covered glacier in the region; and (2) numerically estimate the distributed ice melt rate under the spatially-heterogeneous supraglacial debris of the Batura Glacier. By enhancing our understanding of glacier mass balance behavior and its relationship to debris cover energy budgets in the Karakoram an over the last two decades, this research adds significantly to existing knowledge in this field.

2 Study site

The Batura Glacier, located in northwest Karakoram, stands as one of the most prodigious valley-type glaciers in the lower latitudes, extending over a length of more than 50 km and encompassing an expansive area exceeding 310 km^2 (Xie et al., 2023) (Figure 1). Approximately 24% (~76 km^2) of the glacier's area is covered with debris (Xie et al., 2023), while its thickness in the part below 3000 m a.s.l. surpasses 50 cm (Gao et al., 2020). Influenced by the prevailing Westerlies, the Batura Glacier receives abundant snowfall (exceeding 1000 mm w.e. at altitudes above 5000 meters) in the high-altitude region (Lanzhou Institute of Glaciology and Geocryology, 1980). The glacier is characterized by a relatively lower average air temperature compared to observed glaciers in Tianshan and Himalayas, particularly near the snowline, where frigid temperatures endure throughout the year, averaging

https://doi.org/10.5194/hess-2023-238
Preprint. Discussion started: 6 November 2023

approximately -5℃ annually. The glacier displays a rapid flow velocity, with a maximum rate reaching up to 517.5 m yr^{-1}, facilitated by a high rate of mass turnover, and undergoes frequent periods of advance and retreat, while remaining devoid of any surging events (Bhambri et al., 2017). .

Since the comprehensive investigation on Batura Glacier conducted by Lanzhou Institute of Glaciology and Geocryology during 1974-1975, there has been a scarcity of systematic observations and studies on this glacier. Contemporary investigations of Batura Glacier primarily utilize remote sensing observations, focusing on the glacier dynamics and long-term mass balance, e.g. Rankl and Braun (2016), Wu et al. (2021). There is a challenge in understanding glacier ablation, associated secondary hazards, and the contribution of glacier runoff to river replenishment.

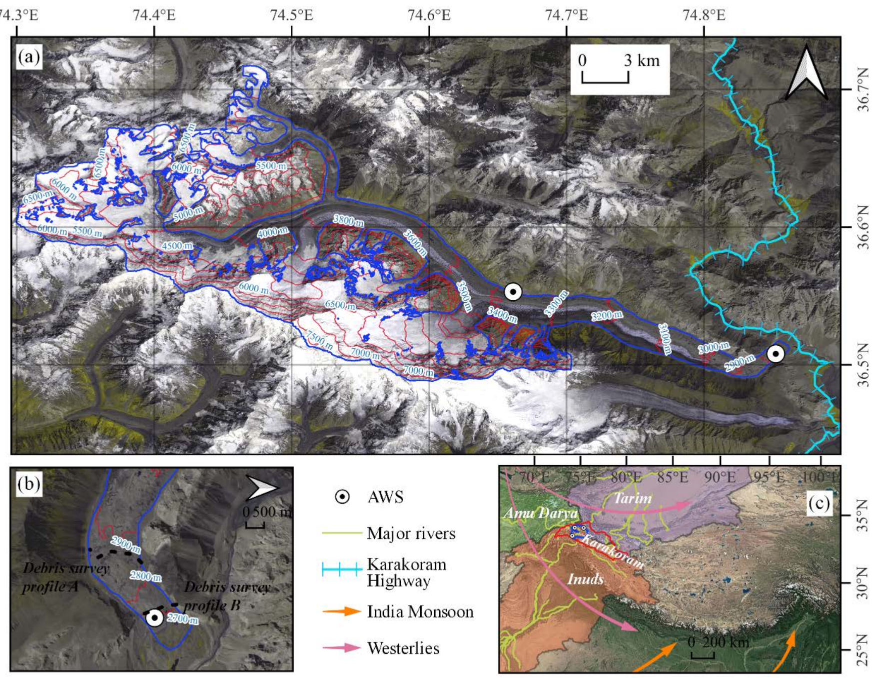

Figure 1 Study area. (a) Topographical conditions of Batura Glacier. (b) Measurement profiles of debris thickness. (c) Geographic location of Batura Glacier, with the red line marked the Karakoram, the blue line indicating the Hunza valley, and Batura situated within the Hunza valley. The three weather stations labeled are Khunjerab, Ziarat, and Naltar.

3 Data and methods

3.1 Data

https://doi.org/10.5194/hess-2023-238
Preprint. Discussion started: 6 November 2023

3.1.1 Observations

An automatic weather station (AWS 1, 74.661° E, 36.550° N, 3390 m) was set up at Batura Glacier on 23 September 2013 by the Northwest Institute of Eco-Environment and Resources, Chinese Academy of Sciences (Figure 1a) and has been in continuous operation since. the location of which is shown in Figure 1. Variables observed at the station are maximum/minimum wind speed and direction, maximum/minimum air temperature, relative humidity, atmospheric pressure, upward and downward long- and shortwave radiation and precipitation, recorded at daily. In this study, we use data from AWS1 in the period 23 September 2013 to 9 May 2018 for the bias correction of HAR v2 (High Asia Refined) reanalysis data(Wang et al., 2020) (see section 3.1.2) and for the accuracy assessment of the energy-mass balance simulations. A second AWS (AWS 2, 74.851° E, 36.506° N, 2664 m) was set up in August 2019 by Yunnan University on a debris-covered part of the tongue of Batura Glacier. Meteorological variables measured consistent with AWS 1 but without precipitation. We use data from AWS 2 between 1 September 2019 to 25 November 2020 in this study to assess the accuracy of parameters for energy balance in the debris-covered area. We additionally used daily maximum/minimum temperatures and precipitation from stations at Khunjerab, Ziarat, and Naltar in the Hunza Valley covering a period from January 1, 1999 to December 31, 2008 to assess the accuracy of HAR in the Hunza basin.

A cross-section of debris thickness data at the terminus of the Batura Glacier (2014) was surveyed by Comsats University Islamabad of Pakistan. Additionally, we collected measurements of debris thickness at six sample points near AWS 2 during in 2019. These data were primarily utilized to validate the simulated surface debris thickness results obtained in this study, based on the methodology proposed by Rounce et al. (2021).

3.1.2 Reanalysis data

The HAR reanalysis data is a product derived from the dynamical downscaling process using the WRF model. The first version of this product was driven by Final operational global analysis (FNL) reanalysis data, while the second version utilized ERA5-atmospheric (0.25°) data (Wang et al., 2020). Compared to the first version, the second version expanded the simulation range and extended the data time and will continue to receive updates (see Wang et al. (2020)). In the production of the meteorological variables, the dynamic assimilation of downscaled results was achieved using satellite products and ground observations such as wind speed, wind direction, temperature, and potential height. This process significantly improved the accuracy and credibility of the downscaling simulation. Notably, the HAR product has shown great potential in reflecting regional water vapor transport processes (Curio et al., 2015) as well as spatial heterogeneity and seasonal variations in precipitation and temperature (Venter et al., 2020).

The meteorological variables in HAR v2 selected to meet the requirements of the energy balance simulation include precipitation, air temperature at 2 m, wind speed (U and V at 10 m), atmospheric pressure, specific humidity, downward shortwave radiation, and cloud cover. The 10 m wind speed was converted to 2 m using an empirical formula provided by Allen et al. (1998), while specific humidity was converted to relative humidity using the formula given by Bolton (1980) utilizing 2 m air temperature and atmospheric pressure.

Temperature was calibrated at the basin scale using a deviation function, which resulted in a range of ±1°C between HAR temperature and station temperature, with a correlation coefficient of 0.98. Details regarding precipitation calibration can be found in section 3.2. Due to the lack of observations for other variables, no further processing was conducted in this study.

3.1.3 Other data

The geodetic mass balance for Batura Glacier generated by Brun et al. (2017), Wu et al. (2020), Shean et al. (2020), Hugonnet et al. (2021) were utilized to validate the energy and mass balance simulation results. These mass balance data were derived from DEM differences with some assumptions such as glacier density, etc. Except for Hugonnet et al. (2021) five-year mass balance (2000-2020), the other data only show the long-term mass balance status after 2000. Time ranges for all mass balance data can be found in Figure. S2. The DEM with a resolution of 30 meters from the Shuttle Radar Topography Mission (SRTM) was used to generate required terrain factors, while the glacier boundary was defined using the most recent result published by Xie et al. (2023).

3.2 Methods

3.2.1 The physically-based energy-mass balance (EMB) model

The EMB model for snow and ice is a distributed model that combines surface energy processes with a subsurface evolution scheme of snow/ice (COSIPY v1.3) which was developed by Sauter et al. (2020). Details of the model relating to applied parametrizations, physical principles and technical infrastructure have been described in Huintjes et al. (2015) and Sauter et al. (2020). In common with previous energy balance models, the surface energy budget is defined as the sum of the net radiation, turbulent heat fluxes (including sensible heat flux q_{sh} and latent heat flux q_{lh}), conductive heat flux (q_g), sensible heat flux of rain (q_{rr}) and melt energy (q_{me}) (Eq.1). The net radiation is the sum of the net shortwave radiation calculated from incoming short radiation ($q_{sw_{in}}$) and surface albedo (α), incoming longwave radiation ($q_{lw_{in}}$) and outcoming longwave radiation ($q_{lw_{out}}$). To link the surface

https://doi.org/10.5194/hess-2023-238
Preprint. Discussion started: 6 November 2023

energy balance to subsurface thermal conduction, the surface temperature (T_s) is defined as an upper Neumann boundary condition. The penetrating energy scheme is based on Bintanja and Van (1995).

$$q_{me} = q_{sw_{in}}(1-\alpha) + q_{lw_{in}} + q_{lw_{out}} + q_{sh} + q_{lh} + q_{rr} + q_g \tag{1}$$

The glacier melt is solved using q_{me} and penetrating energy, while the sublimation is solved using q_{lh}. Combined with the snowfall and refreezing of meltwater (or rain), the total mass balance of glacier can be calculated (Eq2). The sum of subsurface melt (m_{sub}) triggered by penetrating energy and the refreezing of meltwater (or rain) (refreeze), defined as internal mass balance. The internal ablation occurs when temperature at a specific layer reach the melting temperature (T_m). Internal meltwater, in combine with infiltrated surface meltwater, can be stored in the snow layers. Once a layer gets saturated, meltwater will drain into the next layer until the liquid water content within all layers is less than a defined ratio or the meltwater runs off when it reaches the lowest model layer. In this process, a part of meltwater refreezes when temperature at a layer less than T_m. Details for resolving mass and energy budgets can be found in Sauter et al. (2020).

$$mb = \left(\frac{q_{me}}{L_m} + \frac{q_{lh}}{L_v} + \text{snowfall}\right) + (m_{sub} + \text{refreeze}) \tag{2}$$

where L_m is the latent heat of ice melt and L_v is the latent heat of sublimation or condensation.

The debris energy balance is calculated according to the model of Reid and Brock (2010), and the reader is referred to their paper for a detailed description of the model. The sum of energy fluxes at the surface is essentially the same as Eq. 1, but because debris does not melt the debris surface temperature T_s is assumed to change such that these fluxes sum to zero:

$$q_{sw_{in}}(1-\alpha) + q_{lw_{in}}(T_s) + q_{lw_{out}}(T_s) + q_{sh}(T_s) + q_{lh}(T_s) + q_{rr}(T_s) + q_g(T_s) = 0 \tag{3}$$

The circularity in solving for T_s is resolved using a numerical Newton-Raphson method (Eq. 4). Conduction through the debris is then calculated using a Crank-Nicholson scheme with intermediate temperature layers for a set depth, and boundary conditions determined by the newly calculated T_s and the temperature of the debris-ice interface, which is assumed to stay at zero (Eq. 5). The ablation rate is determined from the conductive heat flux to the first ice layer, found using the temperature gradient between the lowest debris layer and the ice (Eq. 6). The detailed solution processes for Eq. 4~6 can be found in Figure 2 and supplementary materials in Reid and Brock (2010).

$$T_s(n+1) = T_s(n) - \frac{fun(T_s(n))}{fun'(T_s(n))'} \tag{4}$$

where, $T_s(n)$ and $fun(T_s(n))$ refer to the temperature and the total energy flux at nth debris layer. The termination condition for this solution is set as $T_s(n+1) - T_s(n) < 0.01$.

https://doi.org/10.5194/hess-2023-238
Preprint. Discussion started: 6 November 2023

$$Q_G = -k_d\left(\frac{dT_s}{dz}\right) \approx k_d \frac{T_s(N-1)-T_m}{h} \quad (5)$$

$$Melt_{deb} = \frac{Q_G}{\rho_i L_f} \quad (6)$$

where, h represents the thickness of each layer, n represents the number of debris layers, and k_d is the thermal conductivity of supraglacial debris. $Melt_{deb}$ refers to ablation under debris.

3.2.2 Model setup and input data

In this study, HAR v2 data were used to drive the model to simulate the energy and mass balance of the Batura Glacier from 2000 to 2020. The inputs were precipitation rate, air temperature, incoming shortwave radiation, cloud cover, air pressure, wind speed, and relative humidity. The simulation was conducted at a spatial resolution of 300m and a temporal step of 1 day. The primary meteorological drivers, such as precipitation and temperature, were calibrated using data from meteorological stations. We employed statistical methods to downscale all meteorological inputs to a resolution of 300m (for more details, please refer to the supplementary methods). The simulation grid was constrained using the glacier boundaries from Xie et al. (2023), and no dynamic adjustments of the glacier were considered.

We utilized the data from Rounce et al. (2021) based on an inversed energy balance modeling procedure as debris thickness input. We validated the simulated debris thickness using observed data, which showed an average deviation of 6 cm. However, it should be noted that the Rounce et al. (2021) results significantly underestimated the debris thickness at certain locations near the terminus of the glacier. For instance, at AWS2, the observed debris thickness was approximately 1.13 m, whereas the inverted thickness was only 0.47 m.

3.2.3 Parameters calibration/ validation

In this study, we use the value ranges for most parameters which have been acquired from empirical equations, large extent observations, and physical processes simulation in previous studies e.g., Reid and Brock (2010), Mölg et al. (2012), Hoffman et al. (2016), Zhu et al. (2020), and Sauter et al. (2020). Given the possible parameter ranges, we have made great effort to obtain the optimal parameter combination. We first determined the values for these physical parameters based on a site-based simulation (AWS1) on Batura Glacier and validated them by identifying the observed outgoing longwave radiation and albedo with the minimum RMSE. The final RMSE between simulations and observations on albedo and outgoing longwave radiation are 0.09 and 18.93 W/m^2, respectively, and there is a high degree of correlation between observations and simulations on annual variations, with correlation coefficients (cc) of 0.83 for albedo and 0.86 for outgoing longwave radiation (Figure S1). Second, we validated the model parameters at for Batura Glacier using geodetic mass balance. The geodetic mass balance agrees well with the simulated mass balance, with an average bias of 0.27 m w.e. at the AWS1 site during different periods (see Figure S2). Particularly, there is a strong agreement between the results from Hugonnet et al. (2021) and our simulations in terms of the trend observed from 2000 to 2020 (Figure S2). This indicates that the parameters used in our study can reliably and accurately estimate the mass and energy budget.

A point simulation at AWS2 was conducted to calibrate and validate the parameters required to simulate energy balance in debris layers. Following Giese et al. (2020), we ascertained the parameters by evaluating the agreement between the simulated surface temperature and the temperature recorded by AWS 2. Figure 2 depicts the comparative analysis of the observed station temperature and the simulated temperature, revealing a commendable consistency between the two over time, exhibiting a correlation coefficient of 0.87. Although there is a tendency to underestimate the temperature in late summer and autumn, and overestimate temperature in late winter. The correlation of observed and simulated temperature for the annual cycle is 0.96, while the RMSE during the simulation period is 0.86 °C. These findings indicate the favorable applicability of the parameterization scheme and parameter values employed for the simulation.

Based on the final parameters determined, the simulated mass balance for the entire glacier is estimated to be -0.23 m w.e.yr^{-1} (2000-2016). It closely aligns with the geodetic mass balances derived from remote sensing (-0.18 m w.e.yr^{-1}, spanning the years 2000-2016, Brun et al. (2017), -0.39 m w.e.yr^{-1}, covering the years 2000-2009, Bolch et al. (2017), and -0.24 m w.e.yr^{-1}, covering the years 2000-2014, Wu et al. (2020)). This further corroborates the reliability of the simulation. The final parameters can be found in Table S1 and S2.

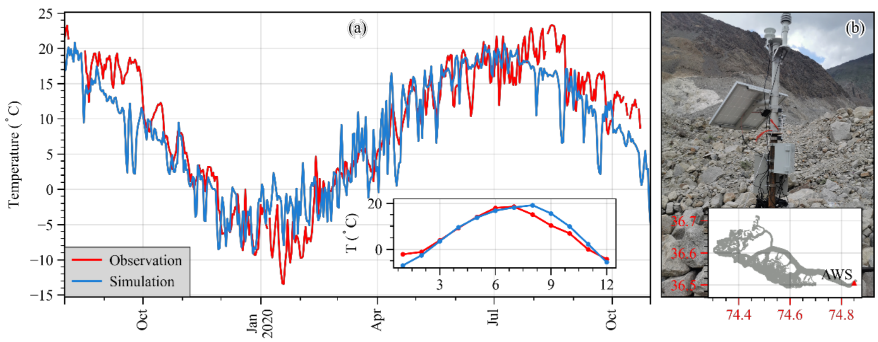

Figure 2 (a) Observed and simulated 2 m air temperature at AWS 2. (b) Photograph and location of AWS2 on Batura Glacier.

https://doi.org/10.5194/hess-2023-238
Preprint. Discussion started: 6 November 2023

4 Results and discussions

4.1 Glacier climatic-mass-balance dynamics and corresponding energy budgets

4.1.1 Mass balance history

The results from the energy balance model show that the average mass balance of the Batura Glacier during the studied period was -0.262 ± 0.561 m w.e. yr^{-1} (Table 1). The glacier experienced its highest positive mass balance in 2010 (0.32 m w.e. yr^{-1}) and its greatest negative mass balance in 2001 (-1.19 m w.e. yr^{-1}). Snowfall was the primary source of glacier mass gain, accounting for 89% of the total mass gain. Refreezing mitigated the internal melting caused by radiation penetration and contributed to 11% of the mass accumulation. Glacier melting constituted 92% of the mass loss, while sublimation/evaporation, which exhibited minimal interannual variability, contributed only 8% to the mass loss.

The model simulations show a decline in glacier ablation after 2008, accompanied by a decrease in the absolute magnitude of the mass budget over the study period (Figure 3a). Independent measurements of thinning rates at the glacier terminus measured by ground radar, declined from 4.58 m yr^{-1} between 1974-2000 to 0.59 m yr^{-1}after 2000 (Gao et al., 2020), implying a similar reducing trend in surface melt rate. This observation further strengthens the alignment with our research results.

As shown in Figure 3b, the variations in internal mass balance and surface mass balance are generally consistent throughout the year, both showing a negative mass balance from June to September. During this period, there was a high shortwave radiation and, consequently, a great amount of snow/ice penetrating radiation occurred. This increased ablation resulted from penetration radiation, coupled with relatively high temperature, reducing the rate of refreezing, and thus causing a negative internal mass balance. The mass budgets in May and October were transitional between accumulation and ablation periods.

https://doi.org/10.5194/hess-2023-238
Preprint. Discussion started: 6 November 2023

Hydrology and Earth System Sciences
Open Access
Discussions

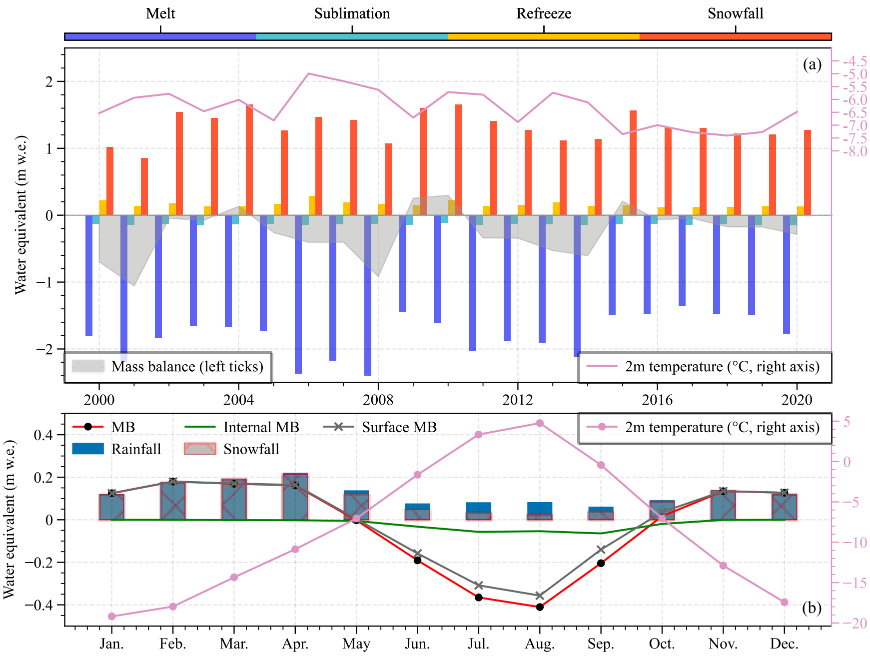

Figure 3 Interannual (upper panel) and mean annual (lower panel) characteristics of the mass components on Batura Glacier over the 2000-2020 study period.

Table 1 Mean values of the mass balance components of Batura glacier from 2000 to 2020.

	Mass balance	Snow accumulation	Refreezing	Surface melt	Sublimation
Values (m w.e. yr^{-1})	-0.262±0.561	1.325±0.174	0.162±0.125	1.613±0.394	0.136±0.005
Proportion of mass gain (loss) (%)	—	89	11	(92)	(8)

Over the study period, the glacier demonstrated a positive rate of annual mass balance change of 0.023 m w.e. yr^{-2}, indicating the glacier's mass balance was becoming less negative and approaching equilibrium between 2000-2020 (Figure 4 a and b). Particularly noteworthy is the trend of decreasing mass loss across the ablation zone, which is particularly pronounced in the higher areas of the tongue and tributary glaciers where debris cover is thin or absent

https://doi.org/10.5194/hess-2023-238
Preprint. Discussion started: 6 November 2023

Hydrology and Earth System Sciences
Discussions
Open Access

(Refer to debris cover Figure S3b), which indicates a reduction in melt (Figure 4a). In contrast, the juncture where debris cover and bare ice meet experienced an increase in the glacier mass balance, suggesting a rise in negative mass balance (negative or balanced in average mass budget during the study period, Figure S3a). Given the rate of mass balance change over time (reduction of melt) is highest in these areas, the mass changes in these areas probably have a large impact on the trend of decreasing negative mass balance.

Across the entire accumulation zone, a slight decrease in mass gain over the 2000-2020 period was observed, with a more pronounced reduction in mass gain observed on the southern flank of the accumulation area, likely linked to diminished winter snowfall. From a mass budget perspective, the glacier's mass balance appears to be approaching equilibrium, likely due to reduced melting during the months of June and July (Figure 4c). For instance, in years characterized by a positive mass balance, such as 2010, the duration of mass accumulation in spring extended, accompanied by minimal mass loss during June and July. The glacier's mass balance generally followed a cyclic pattern spanning roughly five-seven years. However, post-2016, a consistent decline in the glacier's mass balance is evident, possibly indicating a phase of reduced snow accumulation (Figure 4c) gain.

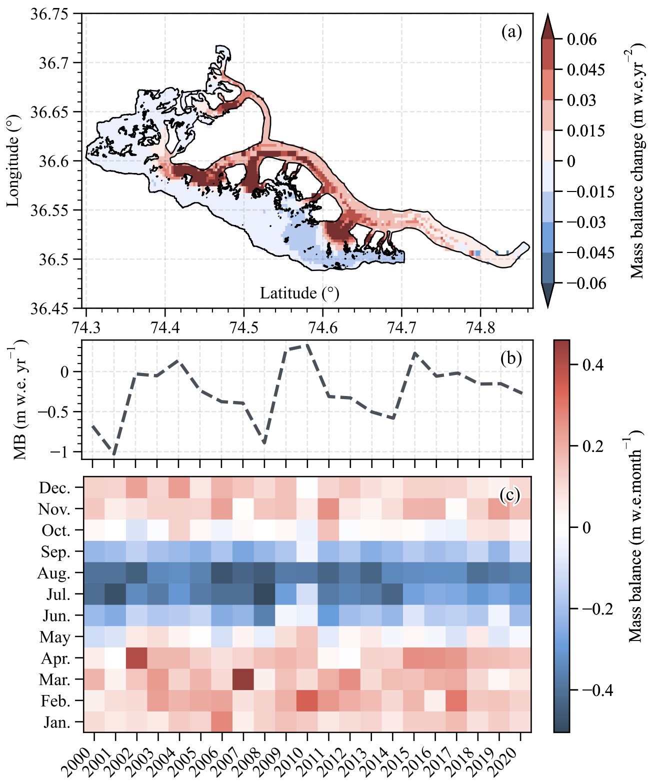

https://doi.org/10.5194/hess-2023-238
Preprint. Discussion started: 6 November 2023

Figure 4 Spatial distribution of the annual mass balance change rate over the 2000-2020 period (a). Time series of modeled annual (b) and monthly (c) mass balance from 2000-2020.

4.1.2 Energy budgets

During 2000-2021, the surface net radiation of the Batura Glacier accounted for the largest proportion of energy heat flux (46%), followed by sensible heat flux (23%), latent heat flux (18%), and conduction heat flux (17%), which made roughly equal contributions.

As presented in Table 2, the net shortwave radiation accounted for 85% of the total energy influx (77 W/m^2), while sensible heat constituted 15% (14 W/m^2). Regarding energy expenditure components, net longwave radiation contributed to 57% (52 W/m^2), melt heat to 20% (18 W/m^2), latent heat to 12% (11 W/m^2), and conductive heat to 11% (10 W/m^2). In terms of the energy components that contribute to glacial mass loss, sublimation latent heat accounted for approximately 38%, while the energy directly responsible for snow/ice melting constituted 62%. For the Batura Glacier, roughly 32% (29 W/m^2 out of 91 W/m^2) of the energy influx was consumed by glacier mass loss, a proportion similar to that of Muztag Ata No.15 Glacier, which was situated in the Westerly influenced area (30%, 26 W/m^2 out of 89 W/m^2) (Zhu et al., 2017). However, it is worth noting that the melting heat of the Batura Glacier was significantly higher than that of Muztag Ata No.15 Glacier (~2 W/m^2), possibly due to disparities in surface debris cover.

During the period of accumulation, a notable proportion of 73% of the energy influx of the Batura Glacier was expended through net longwave radiation, with 15% of the energy utilized for snow/ice sublimation, leaving the remaining portion dedicated to thermal conduction within the debris cover or snow layer. In contrast, throughout the ablation season, the entirety of the energy influx was derived mostly from net shortwave radiation, specifically amounting to 133 W/m^2. The thermal conduction exhibited by the Batura Glacier diverged significantly from debris-free glaciers, such as the Guliya ice cap (Li et al., 2019). In the Batura Glacier, a considerable portion of the energy influx at lower elevations was absorbed by the debris cover, resulting in higher surface temperatures compared to the lower layers, thus yielding negative thermal conduction. Conversely, in the accumulation area, the primary source of energy was dedicated to heating the snow layer. It became evident that during the ablation season, the debris cover assumed a more prominent role, ultimately leading to an overall negative thermal conduction. Among the various components of energy contributing to the glacier mass loss during the ablation period, a significant portion of 69% was attributed to melt heat (33 W/m^2), while the remaining 31% was assigned to sublimation latent heat (15 W/m^2).

https://doi.org/10.5194/hess-2023-238
Preprint. Discussion started: 6 November 2023

Hydrology and Earth System Sciences
Open Access
EGU
Discussions

Table 2 The energy budget on Batura Glacier. All units are W/m^2.

Periods	lw_{in}	lw_{out}	sw_{in}	sw_{out}	$Net\ lw$	$Net\ sw$	Net radiation		sh		lh		g		me
							—	%	—	%	—	%	—	%	
Annual average	212	-264	249	-172	-52	77	25	42	14	23	-11	18	-10	17	18
Ablation (6-9)	231	-293	345	-212	-62	133	71	65	-7	6	-15	14	-16	15	33
Accumulation (10-5)	202	-249	187	-153	-48	34	-12	19	32	52	-10	16	-8	13	0

4.2 Comparations on energy and mass budgets at altitude zones

A significant heterogeneity of mass balance was observed in the Batura Glacier. The mass gain in the glacier accumulation zone can reach up to almost 2 m w.e., whereas terminus melting exceeded 4 m w.e. between 3000-3800 m. Mass balance exhibited distinct altitudinal dependence, whereby the most substantial melting was observed not at the glacier tongue but rather in the range between 3000 and 3400 m (Fig S4a). To elucidate the variations in mass balance across different elevation zones of glaciers, a comparative study was conducted between the Pasu Glacier and the Batura Glacier. The debris-free Pasu glacier is situated adjacent to the Batura Glacier and experiences similar climatic conditions. Consequently, simulations were conducted on the Pasu Glacier using identical parameters.

The equilibrium line altitude (ELA) of the Batura Glacier (4500 m) was significantly higher than that of the Pasu glacier (4150 m). Below the ELA, both glaciers exhibit gentle overall slopes, leading to higher receipt of solar shortwave radiation. As shown in Figure 4, the net radiation of the Batura Glacier was significantly larger than that of the Pasu glacier, primarily attributable to surface albedo disparity. The Pasu Glacier's surface primarily comprises firn or ice, whereas the Batura Glacier is largely covered with fragmented rocks. Evidently, the sensible heat of melt for the Batura Glacier is less than that of the Pasu Glacier, chiefly due to heat conduction between debris layers, which absorb a substantial amount of energy. Overall, the Batura Glacier demonstrated a "bow-shaped" melt energy

https://doi.org/10.5194/hess-2023-238
Preprint. Discussion started: 6 November 2023

pattern from its terminus to the ELA, in sharp contrast to the "slope-increasing" pattern exhibited by the Pasu Glacier. This elevation-linked energy distribution pattern also affects the glaciers' melt characteristics (Figure S4).

Within the regions spanning from the ELA to the zones of maximum snow accumulation (Batura: 4500-5400 m, Pasu: 4150-5400 m), glacier mass accumulated rapidly due to significantly heightened snowfall (Figure S4). Turbulent heat exchange intensifies within this altitude range, with latent heat of melting approaching zero. Limited melting resulted in mass accumulation within the snowpack through refreezing (Figure 5). At altitudes exceeding 5200 m, net radiation, turbulent exchange, and conductive heat flux did not demonstrate significant variation. Net radiation was dominated by longwave radiation, and the snow's surface temperature surpassed the air temperature. The glacier functioned as an energy source, transferring energy to the atmosphere to sustain energy balance, transferring energy to the atmosphere to maintain energy balance. While the maximum snowfall on the Batura Glacier was similar to that on the Pasu Glacier, the accumulating area was larger. For instance, in the region above 7000 m, up to 1 m w.e. of snowfall was observed on the Batura Glacier (Figures S4). Dominated by snowfall and with limited melting, the surface albedo predominantly reflected fresh snow. Changes in precipitation not only induced net radiation variations due to snow albedo feedback but also triggered outgoing longwave radiation and sensible heat variations through alterations in surface temperature. This trait aligned with some of the other glaciers in this area, as well as some glaciers in the West Kunlun and Pamir (Li et al., 2019; Zhu et al., 2017; Bonekamp et al., 2019). However, the Batura Glacier exhibited more negative mass balance compared to these glaciers including the Pasu glacier. Thus, we inferred that the dominant factor shaping the Batura Glacier's mass balance tendency was the impact of low-elevation debris cover on melt latent heat.

Hydrology and Earth System Sciences
Discussions

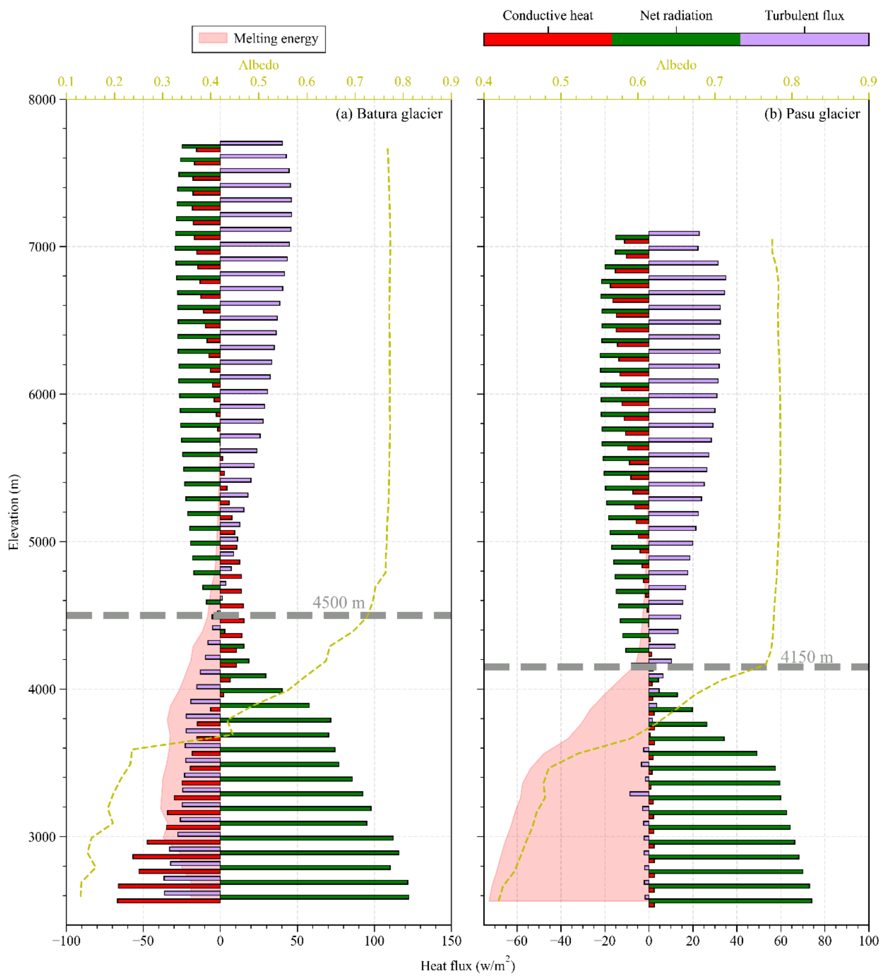

Figure 5 Characteristics of altitude gradient of primary energy components for (a) Batura Glacier and (b) Pasu glacier.

4.3 Impact of debris cover on glacier mass balance

To assess the influence of debris on mass balance, we conducted simulations that compared scenarios with and without supraglacial debris on the Batura Glacier. Our findings revealed that the presence of supraglacial debris led to a notable 45% reduction in the negative mass balance of the Batura Glacier. Specifically, without the presence of debris, the mass balance exhibited a value of -0.48 m w.e. yr^{-1}, while with the inclusion of debris, this value decreased to -0.26 m w.e. yr^{-1}.

https://doi.org/10.5194/hess-2023-238
Preprint. Discussion started: 6 November 2023

Regardless of the time scale, whether on a daily or monthly basis, the impact of supraglacial debris on the Batura Glacier manifested most prominently during the ablation season, as depicted in Figure 6a and 6b. On an interannual scale, supraglacial debris had a significant impact on mass balance of the Batura Glacier; however, it did not induce alterations in its overall fluctuations or trends (Figure 6c). This was mainly because the simulation process did not include the influence of supraglacial debris evolution on mass balance.

The debris had a significant protective effect, effectively mitigating glacier ablation. This effect was most pronounced in August, a period characterized by elevated air temperatures. During May and June an extensive snow cover blanketed the Batura Glacier. When supraglacial debris is included in energy balance processes, the snow layer absorbed a greater amount of heat from the atmosphere through thermal conduction, thereby leading to accelerated melting. As the snow progressively melted and the debris became exposed, the surface albedo experienced a rapid decline spanning from July to October. This transition resulted in the debris absorbing a greater portion of incoming shortwave radiation, much of which is returned to the atmosphere as emitted longwave radiation of sensible heat, consequently yielding a reduction in the melting energy affecting the glacier (Figure 6b). Statistical analysis revealed that when supraglacial debris was not considered, the average net radiation decreased by 14 W/m^2. The most substantial reduction was observed in May, with a reduction of approximately 20 W/m^2.

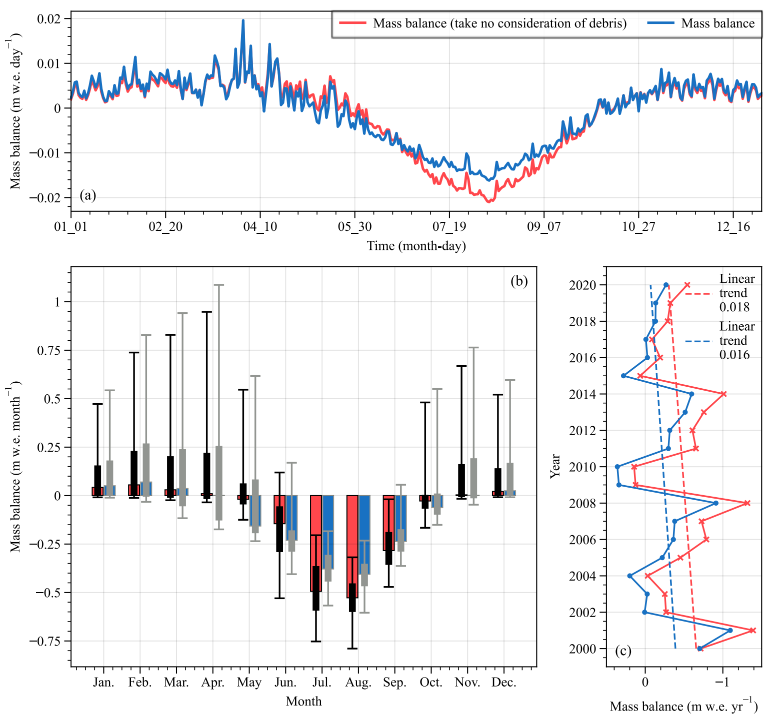

https://doi.org/10.5194/hess-2023-238
Preprint. Discussion started: 6 November 2023

Figure 6 The difference between modeled mass balance with (blue lines and bars) and without debris cover (red lines and bars): (a) daily mass balance; (b) monthly mass balance; and (c) annual mass balance trend.

4.4 The energy controls of sub-debris melt

We conducted additional investigations to understand the mechanisms through which supraglacial debris absorbs and releases energy and consequently mitigates ablation. In the case of the Batura Glacier, the presence of supraglacial debris has the potential to diminish the glacier's albedo, thereby fostering an augmented receipt of net shortwave radiation. Notwithstanding the observed augmentation in net radiation, but an attenuation in melt was recorded. To investigate the impact of debris on energy-driven melting, this study conducted a statistical analysis of the energy balance for scenarios with and without debris coverage in the specific area characterized by the presence of debris (Figure 7). The results illuminated that while the presence of debris did amplify the net radiation income, the available energy for melting is reduced by longwave radiation emission, sensible heat, and thermal conduction within the debris (an average decrease of 25 W/m^2).

During the ablation season (June to September), when accounting for the presence of debris, the glacier's energy income, represented by net shortwave radiation, witnessed an augmentation of 61 W/m^2. Meanwhile, the energy output increased by 116 W/m^2, comprising net longwave radiation (50 W/m^2), sensible heat (42 W/m^2), and conductive heat (24 W/m^2). Consequently, this led to a reduction of 45 W/m^2 in latent heat of melt (sublimation heat of the debris layer, which was not considered when deducting the 11 W/m^2 for sublimation heat without debris cover) (Figure 7). In light of these observations, it can be concluded that the influence of debris cover on glacier melt is twofold. Firstly, it perturbs the turbulent heat exchange processes on the glacier surface. Secondly, it alters the heat flux reaching the glacier through thermal conduction. The former aspect primarily emanates from the heating of the debris layer due to shortwave radiation, causing the debris temperature to surpass the atmospheric temperature. Consequently, the glacier transfers heat to the atmosphere, effectively acting as an energy source. This finding aligns with earlier research results, as exemplified by Steiner et al. (2018) and Nicholson and Stiperski (2020). Regarding the second aspect, we conducted an analysis that considered the thermal conduction occurring within both the debris and ice layer, as well as the energy equilibrium within each layer. When the net radiation was conducted within the debris layers (the radiation penetration of the debris was neglected), it could be consumed to heat the debris, thereby satisfying the energy balance within and between the debris layers.

The process of heat conduction within the debris was clearly illustrated in our study through an analysis of temperature changes within debris of varying thicknesses (Figure 8). During the ablation season, for thinner debris

https://doi.org/10.5194/hess-2023-238
Preprint. Discussion started: 6 November 2023

(Figure 8b, P1), achieving a stable ice surface at absolute zero necessitates a temperature difference of 2.5°C within the uppermost 0.015 m (comprising 3 layers), with an average temperature decrease of 1.7°C per 0.01 m increment. Conversely, in the case of thicker debris (Figure 8f), with a depth of 0.2 m (20 layers), the temperature alteration amounts to 8°C, accompanied by a vertical temperature gradient of 0.4°C per 0.01 m. The variations in temperature are indicative of the attributes associated with sensible heat and conduction heat. Consequently, with respect to the upper layers, thin debris is more likely to conduct a greater amount of heat. At the interface between glaciers and supraglacial debris, the temperature change at P1 (0.035-0.045 m) was 2.5 ℃ with a vertical gradient of 2.5 ℃/0.01m. At P5 (0.42-0.55 m), the vertical gradient of temperature was 0.61 ℃/0.01m. This indicates that in areas covered by thin supraglacial debris, more energy was transferred from the debris to the glacier, resulting in a greater amount of latent heat being released by the glacier.

When the thickness of the debris is comparable, the vertical temperature gradient within the debris exhibits a corresponding similarity (P2, P4), except for slight deviations primarily observed at the surface. These variations are primarily attributed to discrepancies in both air temperature and surface temperature of the debris between the two points. Throughout the accumulation period, net shortwave radiation remained limited, leading to low temperatures and causing the debris temperature to either match or drop below freezing point. As a result, the rate of heat conduction process decelerated, thereby mitigating the influence of the debris on glacier melting.

To quantify the relationship between the thickness (x) of the debris layer and the vertical temperature gradient (y), we computed the average temperature gradient for individual pixels within the debris-covered area during the ablation period and conducted regression analysis (Figure 8g). According to Eq. 7, an increase in debris layer thickness corresponds to a reduction in the vertical temperature gradient. Combined with Eq. 4 & 5, the heat conduction to the interface between the debris layer and the glacier will also decrease, leading to diminished availability of latent heat that contributes to glacier melting. As the thickness of the debris layer approaches minimal values, the heat originating from a temperature difference of approximately 20°C is used for melting. This fundamentally quantifies the impact of debris cover thickness on melt and further explains the differences in mass balance shown in Figure S3.

$$y = -15.35\ln(x) + 36.5(1 - x) \tag{7}$$

https://doi.org/10.5194/hess-2023-238
Preprint. Discussion started: 6 November 2023

Hydrology and Earth System Sciences
Open Access
EGU
Discussions

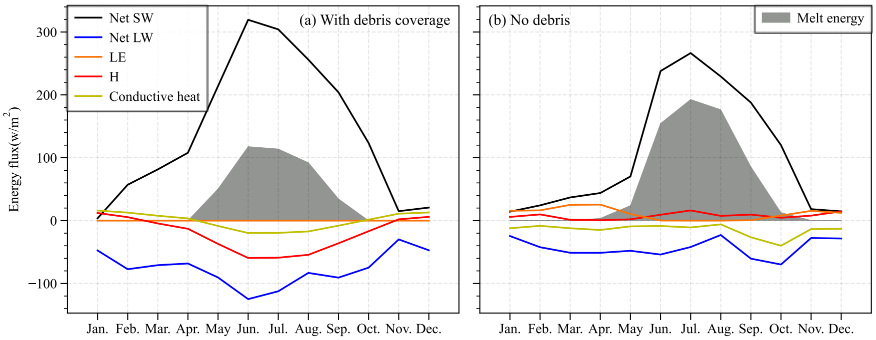

Figure 7 Annual cycles of energy budget (a) with and (b) without debris coverage on Batura Glacier.

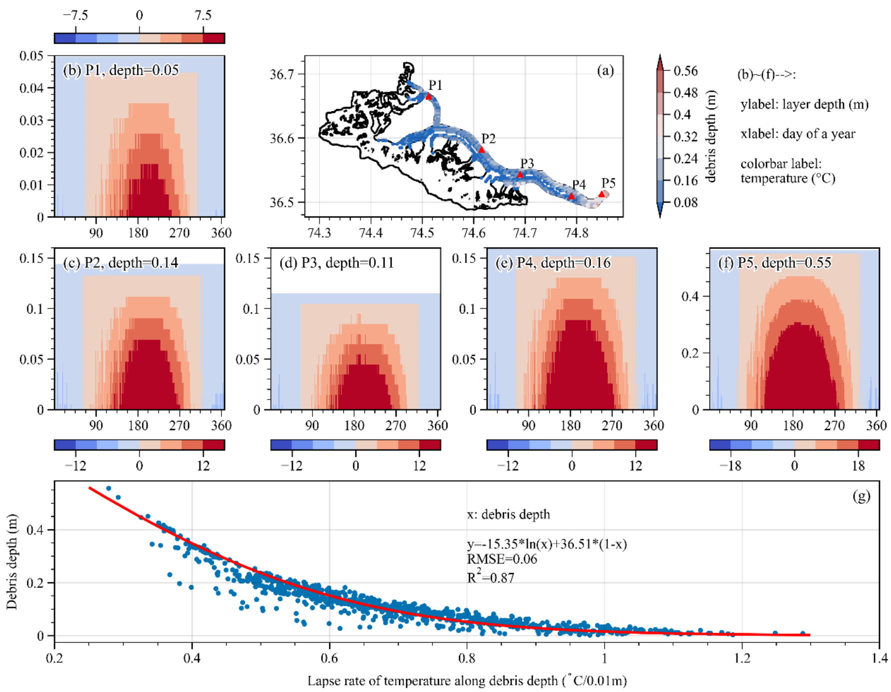

Figure 8 Temporal variations of debris temperature across different depths throughout a year. Temperature profiles at specific points in (a) are displayed in (b)~(f). The relationship between temperature lapse and debris depth is presented in (g).

5 Conclusions and outlook

This study presented a comprehensive investigation into the relationships between supraglacial debris cover, energy fluxes, and mass balance dynamics on the Batura Glacier in the Karakoram. Through analysis and modeling,

https://doi.org/10.5194/hess-2023-238
Preprint. Discussion started: 6 November 2023

we propose that the primary factor influencing the comparatively low negative mass balance of the Batura Glacier is the substantial inhibitory impact exerted by the surface debris on the process of ablation. Furthermore, the glacier's mass budget has shown a decreasing trend in magnitude between 2000 and 2020, primarily due to a reduction in ablation, especially in areas with thin debris cover and debris-free parts of the ablation area, which outweighs the relatively smaller reduction in snowfall accumulation. More detailed findings and viewpoints of the study are concluded as follows.

(1) The Batura Glacier exhibits substantial spatial heterogeneity in mass balance distribution along its elevation gradient. Altitudinal dependence was influenced by the presence of debris cover, resulting in the most intense melting occurring between 3000 and 3400 m, with a reversal of the ablation gradient below 3000 m due to the greater insulation by thicker debris on the lower portion of the glacier.

(2) Our simulations revealed that supraglacial debris cover exerted a notable influence on glacier mass balance. Including debris cover in the energy balance model led to a 45% reduction in the overall mass balance of the Batura Glacier. This reduction was particularly prominent during the ablation season, highlighting the significance of debris cover in mitigating glacier ablation.

(3) The role of debris cover in altering energy exchange was multifaceted. Debris cover enhances net radiation income by reducing albedo but also promotes thermal conduction, which warms the debris and leads to a higher rate of energy transfer to the atmosphere through longwave emission and sensible heat, thereby moderating latent heat of melting. This intricate interplay modified the glacier's response to energy budgets, ultimately affecting its mass balance.

(4) Our investigation into the effects of debris thickness on temperature gradients within the debris layer reveals a fundamental connection between debris thickness and its influence on melt processes. Thicker debris layers engender reduced temperature gradients, leading to diminished latent heat available for glacier melting.

This study significantly advances our understanding of energy and mass interaction on debris-covered glaciers in the Karakoram. However, further work is needed to improve our understanding of glacier anomalies in this region. First, future work should consider the evolution of supraglacial debris thickness, as changes in this thickness have a significant impact on the energy reaching the glacier surface. Second, glacier dynamics should be considered in the simulations, and more remote sensing products such as glacier flow velocity should be added to constrain the different processes of the model. Finally, this paper has pointed out that the mass balance of Batura Glacier is

Hydrology and Earth System Sciences Discussions

becoming less negative, which is an interesting phenomenon linking with the "Karakoram anomaly" and should be further discussed and investigation.

The contact author has declared that none of the authors has any competing interests.

Acknowledgments

The authors acknowledge financial support from the National Natural Science Foundation of China (Nos. 42301154 and 42171129), the National Key R&D Program International Science and Technology Innovation Cooperation Project (No. 2023YFE0102800), and the Postdoctoral Research Foundation of Yunnan Province (No. C615300504038).

References

Allen, R., Pereira, L., Raes, D., Smith, M., Allen, R. G., Pereira, L. S., and Martin, S.: Crop Evapotranspiration: Guidelines for Computing Crop Water Requirements, FAO Irrigation and Drainage Paper 56, FAO, 56, 1998.

Azam, M. F., Wagnon, P., Berthier, E., Vincent, C., Fujita, K., and Kargel, J. S.: Review of the status and mass changes of Himalayan-Karakoram glaciers, Journal of Glaciology, 64, 61-74, 10.1017/jog.2017.86, 2018.

Banerjee, A.: Brief communication: Thinning of debris-covered and debris-free glaciers in a warming climate, The Cryosphere, 11, 133-138, 10.5194/tc-11-133-2017, 2017.

Basnett, S., Kulkarni, A. V., and Bolch, T.: The influence of debris cover and glacial lakes on the recession of glaciers in Sikkim Himalaya, India, Journal of Glaciology, 59, 1035-1046, 10.3189/2013JoG12J184, 2013.

Bhambri, R., Hewitt, K., Kawishwar, P., and Pratap, B.: Surge-type and surge-modified glaciers in the Karakoram, Sci Rep, 7, 15391, 10.1038/s41598-017-15473-8, 2017.

Bintanja, R. and Van, D. B., Michiel R.: The Surface Energy Balance of Antarctic Snow and Blue Ice, Journal of Applied Meteorology, 34, 902-926, 1995.

Bisset, R. R., Dehecq, A., Goldberg, D. N., Huss, M., Bingham, R. G., and Gourmelen, N.: Reversed Surface-Mass-Balance Gradients on Himalayan Debris-Covered Glaciers Inferred from Remote Sensing, Remote Sensing, 12, 10.3390/rs12101563, 2020.

Bolch, T., Pieczonka, T., Mukherjee, K., and Shea, J.: Brief communication: Glaciers in the Hunza catchment (Karakoram) have been nearly in balance since the 1970s, The Cryosphere, 11, 531-539, 10.5194/tc-11-531-2017, 2017.

Bolton, D.: The Computation of Equivalent Potential Temperature, Monthly Weather Review, 108, 1046-1053, 1980.

Bonekamp, P. N. J., de Kok, R. J., Collier, E., and Immerzeel, W. W.: Contrasting Meteorological Drivers of the Glacier Mass Balance Between the Karakoram and Central Himalaya, Frontiers in Earth Science, 7, 10.3389/feart.2019.00107, 2019.

Brun, F., Berthier, E., Wagnon, P., Kaab, A., and Treichler, D.: A spatially resolved estimate of High Mountain Asia glacier mass balances, 2000-2016, Nat Geosci, 10, 668-673, https://doi.org/10.1038/NGEO2999, 2017.

Collier, E., Maussion, F., Nicholson, L. I., Mölg, T., Immerzeel, W. W., and Bush, A. B. G.: Impact of debris cover on glacier ablation and atmosphere–glacier feedbacks in the Karakoram, The Cryosphere, 9, 1617-1632, 10.5194/tc-9-1617-2015, 2015.

Collier, E., Nicholson, L. I., Brock, B. W., Maussion, F., Essery, R., and Bush, A. B. G.: Representing moisture fluxes and phase changes in glacier debris cover using a reservoir approach, The Cryosphere, 8, 1429-1444, 10.5194/tc-8-1429-2014, 2014.

Curio, J., Maussion, F., and Scherer, D.: A 12-year high-resolution climatology of atmospheric water transport over the Tibetan Plateau, Earth System Dynamics, 6, 109-124, 10.5194/esd-6-109-2015, 2015.
Evatt, G. W., Abrahams, I. D., Heil, M., Mayer, C., Kingslake, J., Mitchell, S. L., Fowler, A. C., and Clark, C. D.: Glacial melt under a porous debris layer, Journal of Glaciology, 61, 825-836, 10.3189/2015JoG14J235, 2015.
Fujita, K. and Sakai, A.: Modelling runoff from a Himalayan debris-covered glacier, Hydrology and Earth System Sciences, 18, 2679-2694, 10.5194/hess-18-2679-2014, 2014.
Gao, H., Zou, X., Wu, J., Zhang, Y., Deng, X., Hussain, S., Wazir, M. A., and Zhu, G.: Post-20(th) century near-steady state of Batura Glacier: observational evidence of Karakoram Anomaly, Sci Rep, 10, 987, 10.1038/s41598-020-57660-0, 2020.
Gardelle, J., Berthier, E., and Arnaud, Y.: Slight mass gain of Karakoram glaciers in the early twenty-first century, Nature Geoscience, 5, 322-325, 10.1038/ngeo1450, 2012.
Giese, A., Boone, A., Wagnon, P., and Hawley, R.: Incorporating moisture content in surface energy balance modeling of a debris-covered glacier, The Cryosphere, 14, 1555-1577, 10.5194/tc-14-1555-2020, 2020.
Hewitt, K.: The Karakoram Anomaly? Glacier Expansion and the ‘Elevation Effect,’ Karakoram Himalaya, Mountain Research and Development, 25, 332-340, 10.1659/0276-4741(2005)025[0332:tkagea]2.0.co;2, 2005.
Hoffman, M. J., Fountain, A. G., and Liston, G. E.: Distributed modeling of ablation (1996–2011) and climate sensitivity on the glaciers of Taylor Valley, Antarctica, Journal of Glaciology, 62, 215-229, 10.1017/jog.2015.2, 2016.
Hugonnet, R., McNabb, R., Berthier, E., Menounos, B., Nuth, C., Girod, L., Farinotti, D., Huss, M., Dussaillant, I., Brun, F., and Kaab, A.: Accelerated global glacier mass loss in the early twenty-first century, Nature, 592, 726-731, https://doi.org/10.1038/s41586-021-03436-z, 2021.
Huintjes, E., Sauter, T., Schröter, B., Maussion, F., Yang, W., Kropáček, J., Buchroithner, M., Scherer, D., Kang, S., and Schneider, C.: Evaluation of a Coupled Snow and Energy Balance Model for Zhadang Glacier, Tibetan Plateau, Using Glaciological Measurements and Time-Lapse Photography, Arctic, Antarctic, and Alpine Research, 47, 573-590, 10.1657/aaar0014-073, 2015.
Huo, D., Bishop, M. P., Young, B., and Chi, Z.: Modeling the feedbacks between surface ablation and morphological variations on debris-covered Baltoro Glacier in the central Karakoram, Geomorphology, 389, 10.1016/j.geomorph.2021.107840, 2021.
Juen, M., Mayer, C., Lambrecht, A., Han, H., and Liu, S.: Impact of varying debris cover thickness on ablation: a case study for Koxkar Glacier in the Tien Shan, The Cryosphere, 8, 377-386, 10.5194/tc-8-377-2014, 2014.
Kääb, A., Berthier, E., Nuth, C., Gardelle, J., and Arnaud, Y.: Contrasting patterns of early twenty-first-century glacier mass change in the Himalayas, Nature, 488, 495-498, https://doi.org/10.1038/nature11324, 2012.
Lanzhou Institute of Glaciology and Geocryology, C. A. o. S.: Studies and investigations on the Batura Glacier, Karakoram, China Science Publishing & Media Ltd, Beijing1980.
Li, S., Yao, T., Yu, W., Yang, W., and Zhu, M.: Energy and mass balance characteristics of the Guliya ice cap in the West Kunlun Mountains, Tibetan Plateau, Cold Regions Science and Technology, 159, 71-85, https://doi.org/10.1016/j.coldregions.2018.12.001, 2019.
Mayer, C., Lambrecht, A., Oerter, H., Schwikowski, M., Vuillermoz, E., Frank, N., and Diolaiuti, G.: Accumulation Studies at a High Elevation Glacier Site in Central Karakoram, Advances in Meteorology, 2014, 1-12, 10.1155/2014/215162, 2014.
Mihalcea, C., Mayer, C., Diolaiuti, G., D’Agata, C., Smiraglia, C., Lambrecht, A., Vuillermoz, E., and Tartari, G.: Spatial distribution of debris thickness and melting from remote-sensing and meteorological data, at debris-covered Baltoro glacier, Karakoram, Pakistan, Annals of Glaciology, 48, 49-57, 10.3189/172756408784700680, 2008.
Mölg, N., Bolch, T., Rastner, P., Strozzi, T., and Paul, F.: A consistent glacier inventory for Karakoram and Pamir derived from Landsat data: distribution of debris cover and mapping challenges, Earth System Science Data, 10, 1807-1827,

10.5194/essd-10-1807-2018, 2018.

Mölg, T., Maussion, F., Yang, W., and Scherer, D.: The footprint of Asian monsoon dynamics in the mass and energy balance of a Tibetan glacier, The Cryosphere, 6, 1445-1461, 10.5194/tc-6-1445-2012, 2012.

Muhammad, S., Tian, L., Ali, S., Latif, Y., Wazir, M. A., Goheer, M. A., Saifullah, M., Hussain, I., and Shiyin, L.: Thin debris layers do not enhance melting of the Karakoram glaciers, Sci Total Environ, 746, 141119, 10.1016/j.scitotenv.2020.141119, 2020.

Nicholson, L. and Benn, D. I.: Calculating ice melt beneath a debris layer using meteorological data, Journal of Glaciology, 52, 463-470, 2006.

Nicholson, L. and Stiperski, I.: Comparison of turbulent structures and energy fluxes over exposed and debris-covered glacier ice, Journal of Glaciology, 66, 543-555, 10.1017/jog.2020.23, 2020.

Nie, Y., Pritchard, H. D., Liu, Q., Hennig, T., Wang, W., Wang, X., Liu, S., Nepal, S., Samyn, D., Hewitt, K., and Chen, X.: Glacial change and hydrological implications in the Himalaya and Karakoram, Nature Reviews Earth & Environment, 10.1038/s43017-020-00124-w, 2021.

Nuimura, T., Fujita, K., and Sakai, A.: Downwasting of the debris-covered area of Lirung Glacier in Langtang Valley, Nepal Himalaya, from 1974 to 2010, Quaternary International, 455, 93-101, 10.1016/j.quaint.2017.06.066, 2017.

östrem, G.: Ice Melting under a Thin Layer of Moraine, and the Existence of Ice Cores in Moraine Ridges, Geografiska Annaler, 41, 228-230, 10.1080/20014422.1959.11907953, 1959.

Rankl, M. and Braun, M.: Glacier elevation and mass changes over the central Karakoram region estimated from TanDEM-X and SRTM/X-SAR digital elevation models, Annals of Glaciology, 57, 273-281, 10.3189/2016AoG71A024, 2016.

Reid, T. D. and Brock, B. W.: An energy-balance model for debris-covered glaciers including heat conduction through the debris layer, Journal of Glaciology, 56, 903-916, 2010.

Rounce, D. R., Hock, R., McNabb, R. W., Millan, R., Sommer, C., Braun, M. H., Malz, P., Maussion, F., Mouginot, J., Seehaus, T. C., and Shean, D. E.: Distributed Global Debris Thickness Estimates Reveal Debris Significantly Impacts Glacier Mass Balance, Geophys Res Lett, 48, e2020GL091311, 10.1029/2020GL091311, 2021.

Sauter, T., Arndt, A., and Schneider, C.: COSIPY v1.3 – an open-source coupled snowpack and ice surface energy and mass balance model, Geoscientific Model Development, 13, 5645-5662, 10.5194/gmd-13-5645-2020, 2020.

Shean, D. E., Bhushan, S., Montesano, P., Rounce, D. R., Arendt, A., and Osmanoglu, B.: A Systematic, Regional Assessment of High Mountain Asia Glacier Mass Balance, Frontiers in Earth Science, 7, https://doi.org/10.3389/feart.2019.00363, 2020.

Steiner, J. F., Litt, M., Stigter, E. E., Shea, J., Bierkens, M. F. P., and Immerzeel, W. W.: The Importance of Turbulent Fluxes in the Surface Energy Balance of a Debris-Covered Glacier in the Himalayas, Frontiers in Earth Science, 6, 10.3389/feart.2018.00144, 2018.

Venter, Z. S., Brousse, O., Esau, I., and Meier, F.: Hyperlocal mapping of urban air temperature using remote sensing and crowdsourced weather data, Remote Sensing of Environment, 242, 10.1016/j.rse.2020.111791, 2020.

Wang, X., Tolksdorf, V., Otto, M., and Scherer, D.: WRF-based dynamical downscaling of ERA5 reanalysis data for High Mountain Asia: Towards a new version of the High Asia Refined analysis, International Journal of Climatology, 41, 743-762, 10.1002/joc.6686, 2020.

Wu, K., Liu, S., Jiang, Z., Liu, Q., Zhu, Y., Yi, Y., Xie, F., Ahmad Tahir, A., and Saifullah, M.: Quantification of glacier mass budgets in the Karakoram region of Upper Indus Basin during the early twenty-first century, Journal of Hydrology, 603, 10.1016/j.jhydrol.2021.127095, 2021.

Wu, K., Liu, S., Jiang, Z., Zhu, Y., Xie, F., Gao, Y., Yi, Y., Tahir, A. A., and Muhammad, S.: Surging Dynamics of Glaciers in the Hunza Valley under an Equilibrium Mass State since 1990, Remote Sensing, 12, 10.3390/rs12182922, 2020.

Xie, F., Liu, S., Wu, K., Zhu, Y., Gao, Y., Qi, M., Duan, S., Saifullah, M., and Tahir, A. A.: Upward Expansion of Supra-

Glacial Debris Cover in the Hunza Valley, Karakoram, During 1990 ~ 2019, Frontiers in Earth Science, 8, 10.3389/feart.2020.00308, 2020.

Xie, F., Liu, S., Gao, Y., Zhu, Y., Bolch, T., Kääb, A., Duan, S., Miao, W., Kang, J., Zhang, Y., Pan, X., Qin, C., Wu, K., Qi, M., Zhang, X., Yi, Y., Han, F., Yao, X., Liu, Q., Wang, X., Jiang, Z., Shangguan, D., Zhang, Y., Grünwald, R., Adnan, M., Karki, J., and Saifullah, M.: Interdecadal glacier inventories in the Karakoram since the 1990s, Earth System Science Data, 15, 847-867, 10.5194/essd-15-847-2023, 2023.

Zemp, M., Huss, M., Thibert, E., Eckert, N., McNabb, R., Huber, J., Barandun, M., Machguth, H., Nussbaumer, S. U., Gartner-Roer, I., Thomson, L., Paul, F., Maussion, F., Kutuzov, S., and Cogley, J. G.: Global glacier mass changes and their contributions to sea-level rise from 1961 to 2016, Nature, 568, 382-386, 10.1038/s41586-019-1071-0, 2019.

Zhu, M., Yao, T., Xie, Y., Xu, B., Yang, W., and Yang, S.: Mass balance of Muji Glacier, northeastern Pamir, and its controlling climate factors, Journal of Hydrology, 590, 10.1016/j.jhydrol.2020.125447, 2020.

Zhu, M., Yao, T., Yang, W., Xu, B., Wu, G., and Wang, X.: Differences in mass balance behavior for three glaciers from different climatic regions on the Tibetan Plateau, Climate Dynamics, 50, 3457-3484, 10.1007/s00382-017-3817-4, 2017.